

Antiferromagnetic ordering in the Kondo lattice system $\text{Yb}_2\text{Fe}_3\text{Si}_5$

Yogesh Singh and S. Ramakrishnan

Tata Institute of Fundamental Research, Mumbai-400005, India

Z. Hossain and C. Geibel

Max-Planck-Institute for Chemical Physics of Solids, D-01187 Dresden, Germany

(Received 11 January 2002; published 1 July 2002)

Compounds belonging to the $R_2\text{Fe}_3\text{Si}_5$ series exhibit unusual superconducting and magnetic properties. Although a number of studies have been made on the first reentrant antiferromagnet superconductor $\text{Tm}_2\text{Fe}_3\text{Si}_5$, the physical properties of $\text{Yb}_2\text{Fe}_3\text{Si}_5$ are largely unexplored. In this work, we attempt to provide a comprehensive study of bulk properties such as, resistivity, susceptibility, and heat capacity of a well-characterized polycrystalline $\text{Yb}_2\text{Fe}_3\text{Si}_5$. Our measurements indicate that Yb^{3+} moments order antiferromagnetically below 1.7 K. Moreover, the system behaves as a Kondo lattice with large Sommerfeld coefficient (γ) of 0.5 J/Yb mol K^2 at 0.3 K, which is well below T_N . The absence of superconductivity in $\text{Yb}_2\text{Fe}_3\text{Si}_5$ down to 0.3 K at ambient pressure is attributed to the presence of the Kondo effect.

DOI: 10.1103/PhysRevB.66.014415

PACS number(s): 72.10.Fk, 72.15.Qm, 75.20.Hr, 75.30.Mb

I. INTRODUCTION

Ternary rare-earth transition metal silicides, which form in a variety of crystal structures have been widely investigated due to their remarkable physical properties.^{1,2} A few of them also undergo superconducting transition at low temperatures.^{3,4} In the early 1980's, several investigations have been carried out to understand the superconductivity and magnetism exhibited by compounds belonging to the $R_2\text{Fe}_3\text{Si}_5$ system.⁵⁻⁸ In this family the Fe atoms do not carry any magnetic moment but help in building a large density of states at the Fermi level.⁹ It is now well established that a member of this series, namely, $\text{Tm}_2\text{Fe}_3\text{Si}_5$ (Ref. 10) is the first reentrant antiferromagnetic superconductor (perhaps the only one down to 50 mK). It is worthwhile to point out that we still do not know why the antiferromagnetic order among Tm^{3+} ions is a deterrent to the superconductivity in $\text{Tm}_2\text{Fe}_3\text{Si}_5$ given that the neutron scattering studies¹⁰ could not find any ferromagnetic component in the magnetic unit cell in this compound. A recent report has suggested that an antiferromagnet $\text{Er}_2\text{Fe}_3\text{Si}_5$ (Ref. 11) (below 2.5 K) also shows superconductivity below 1 K whereas an earlier heat-capacity study⁸ indicated quadruple magnetic transitions without any superconductivity down to 1.5 K. A previous study⁸ on an arc melted $\text{Yb}_2\text{Fe}_3\text{Si}_5$ sample reported the observation of antiferromagnetic ordering of Yb moments around 1.7 K. However, that study did neither establish the Kondo lattice behavior nor the high value of the Sommerfeld coefficient (γ) as we will see later. In this context, the physical properties of $\text{Yb}_2\text{Fe}_3\text{Si}_5$ are largely unexplored as compared to other compounds of the $R_2\text{Fe}_3\text{Si}_5$ series. Moreover, compounds with magnetic trivalent or nearly trivalent Yb are interesting since valence instability and Kondo interaction can lead to unusual properties. Thus, we need to understand the absence of superconductivity in Yb compound given that both Tm and Lu of the same series exhibit superconductivity. In this work, we provide a comprehensive study of bulk

properties such as, resistivity, susceptibility, and heat capacity of a well characterized polycrystalline sample of $\text{Yb}_2\text{Fe}_3\text{Si}_5$.

II. EXPERIMENTAL DETAILS

Samples of $\text{Yb}_2\text{Fe}_3\text{Si}_5$ were made by melting the individual constituents (with 2% Yb excess and other elements taken in stoichiometric proportions) in an alumina crucible which is placed inside a tantalum container and sealed in an arc furnace under high purity argon atmosphere. The whole assembly is heated in a vertical furnace. The purity of the rare-earth element Yb and the transition element Fe were 99.99% whereas the purity of Si was 99.999%. The mixture was heated to about 900 °C for an hour and then it was heated 1600 °C for 20 min. Subsequently, the mixture is cooled slowly to room temperature. The x-ray powder diffraction pattern of the sample did not show the presence of any parasitic impurity phases. The quality of the sample was checked with EDAX analysis confirming that the sample is essentially single phase with 2-3-5 composition. The unit cell of the tetragonal structure ($\text{Sc}_2\text{Fe}_3\text{Si}_5$ -type, space group $P4/mnc$) is shown in Fig. 1. The basic structure of the $R_2\text{Fe}_3\text{Si}_5$ compounds is derived from BaAl_4 -type structure. They form in the tetragonal structure in which two different sets of Fe sites are present, one type [Fe(2)] forming chains along [001] direction, a second type [Fe(1)] forming isolated squares parallel to the basal plane. The nearest rare-earth distances in $\text{Yb}_2\text{Fe}_3\text{Si}_5$ is 3.8 Å. The crystal structure of the given sample was refined using FULLPROF¹² and the result is shown in Fig. 2. The slight difference in the intensity profile is probably associated with preferred orientation effects which have not been taken into account in the present analysis. The refined lattice constants along with the unit cell parameters are given in Table I.

The temperature dependence of the magnetic susceptibility (χ) was measured using the commercial SQUID magneto-

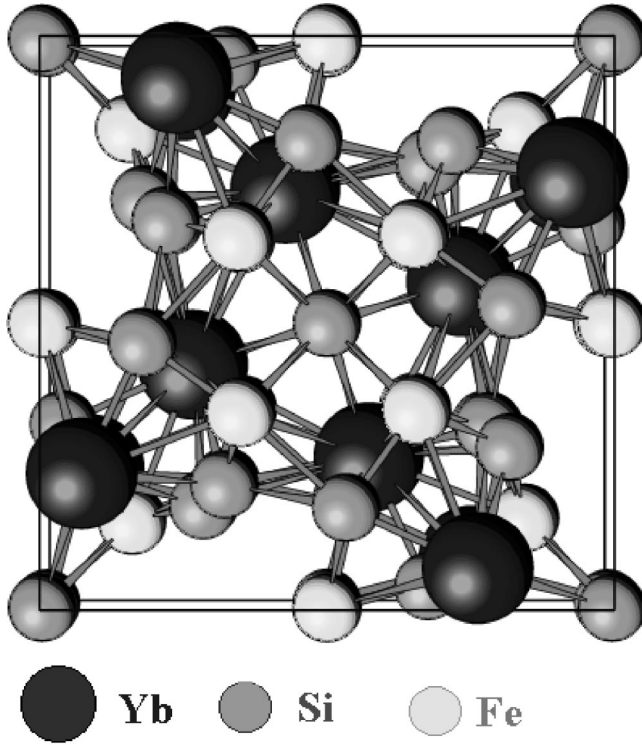


FIG. 1. Structure of the unit cell of $\text{Yb}_2\text{Fe}_3\text{Si}_5$ which forms in the tetragonal $\text{Sc}_2\text{Fe}_3\text{Si}_5$ type structure (space group $P4/mnc$) as viewed along the c axis.

meter (MPMS5, Quantum Design, USA) in a field of 1 kOe in the temperature range from 1.9 to 300 K. The ac susceptibility was measured using a home built susceptometer¹³ from 1.5 to 20 K. The resistivity was measured using a four-

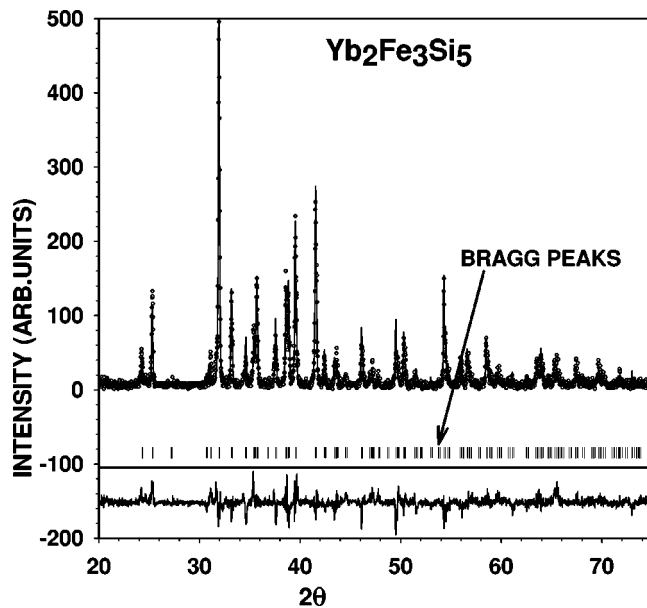


FIG. 2. Observed and fitted x-ray power diffraction pattern of $\text{Yb}_2\text{Fe}_3\text{Si}_5$ using the FULLPROF program. The vertical bars mark the Bragg peaks and the difference between observed and calculated intensity is also plotted below.

TABLE I. Unit cell parameters obtained from the FULLPROF refinement of the powder x-ray diffraction data of $\text{Yb}_2\text{Fe}_3\text{Si}_5$. $a = 10.3537(5)$ Å and $c = 5.3855(5)$ Å.

| Atom | Z | Wyck | x | y | z |
|------|----|------|---------|---------|---------|
| Yb | 70 | 8h | 0.07411 | 0.23910 | 0.00000 |
| Fe | 26 | 4d | 0.00000 | 0.50000 | 0.25000 |
| Fe | 26 | 8h | 0.34940 | 0.34510 | 0.00000 |
| Si | 14 | 4e | 0.00000 | 0.00000 | 0.25570 |
| Si | 14 | 8h | 0.18000 | 0.71710 | 0.25000 |
| Si | 14 | 8h | 0.17910 | 0.46640 | 0.00000 |

probe dc technique with contacts made using silver paint on a bar shaped sample of 1 mm thick, 10 mm length, and 2 mm width. The temperature was measured using a calibrated Si diode (Lake Shore Inc., USA) sensor. The sample voltage was measured with a nanovoltmeter (model 182, Keithley, USA) with a current of 10 mA using a 20 ppm stable (Hewlett Packard, USA) current source. All the data were collected using an IBM compatible PC/AT via IEEE-488 interface. The heat-capacity in zero field between 0.3 to 30 K was measured using an automated adiabatic heat pulse method. A calibrated germanium resistance thermometer (Lake Shore Inc, USA) was used as the temperature sensor in this range.

III. RESULTS

A. Magnetic susceptibility studies

The temperature dependence of the inverse dc magnetic susceptibility ($1/\chi_{dc}$) of a polycrystalline $\text{Yb}_2\text{Fe}_3\text{Si}_5$ in a field of 1 kOe from 1.9 to 300 K is shown in the Fig. 3. The high-temperature susceptibility ($100 \text{ K} < T < 300 \text{ K}$) is fitted to a modified Curie-Weiss expression which is given by

$$\chi = \chi_0 + \frac{C}{(T - \theta_p)}. \quad (1)$$

Here, χ_0 is the temperature independent susceptibility (sum of Pauli, Landau, and core susceptibilities), C is the Curie constant, and θ_p is the Curie-Weiss temperature. The Curie constant C can be written in terms of the effective moment as

$$C = \frac{\mu_{\text{eff}}^2 x}{8}, \quad (2)$$

where x is the concentration of Yb^{3+} ions ($x=2$ for $\text{Yb}_2\text{Fe}_3\text{Si}_5$). The value of $\chi(0)$ is extremely small (7×10^{-4} emu/mol) while the values of the effective magnetic moment (μ_{eff}) and θ_p are found to be $4.5\mu_B$ and -14.4 K , respectively. The estimated effective moment is found to be nearly equal to the free ion moment of the magnetic Yb^{3+} ion which rules out the possibility of mixed valent nature of Yb as conjectured in an earlier study.⁸ One can also observe that below 100 K, the χ data show deviation from Curie-Weiss plot which could be due to the combined effect of

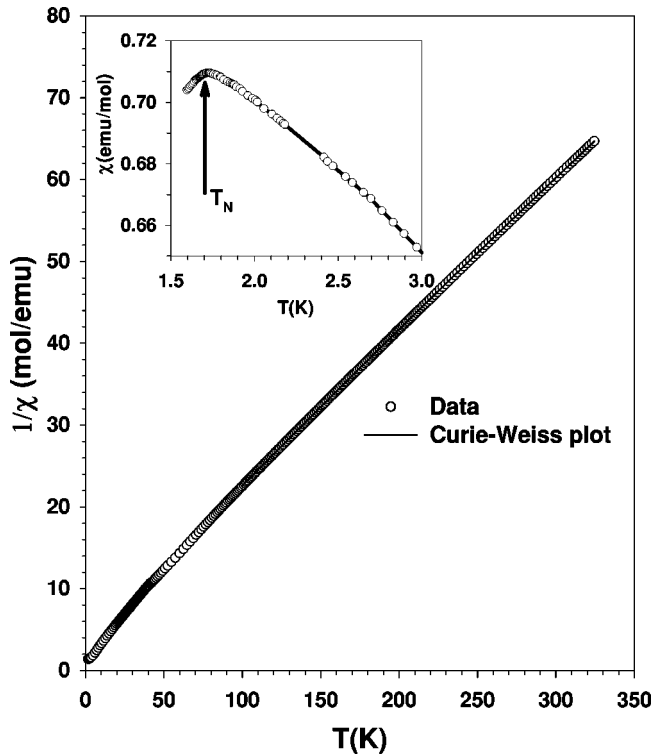


FIG. 3. Temperature dependence of the inverse susceptibility ($1/\chi_{dc}$) of $\text{Yb}_2\text{Fe}_3\text{Si}_5$ in a field of 1 kOe from 1.9 to 300 K. The inset shows the low temperature ac χ data of $\text{Yb}_2\text{Fe}_3\text{Si}_5$, which displays the antiferromagnetic transition at 1.7 K. The solid line is a fit to the Curie-Weiss relation (see text).

crystal field and Kondo lattice contributions. The inset shows the ac-susceptibility behavior of the sample at low temperature. This inset clearly indicates antiferromagnetic ordering of Yb^{3+} moments at 1.7 K. It must be emphasized here that we do not see the influence of any impurity contribution to $\chi(T)$ and especially the absence of Yb_2O_3 ($T_N=2.3$ K) which is generally present in many Yb based compounds. The presence of a single distinct anomaly in χ at 1.7 K clearly suggests the high quality of the sample.

Earlier study⁸ showed that the antiferromagnetic ordering temperature of the heavy rare-earth $R_2\text{Fe}_3\text{Si}_5$ compounds do follow the de Gennes scaling¹⁴ [$\sim (g_J - 1)^2 J(J + 1)$] indicating that the dominant magnetic interaction is the RKKY interaction. But the same study revealed that the antiferromagnetic ordering temperature of $\text{Yb}_2\text{Fe}_3\text{Si}_5$ lies far above the theoretical curve.⁸ However, an antiferromagnetic ordering temperature of 1.7 K is a very common value for Yb compounds. A slightly enhanced $4f$ hybridization, in addition to inducing some Kondo interaction, leads at first to an increase of the magnetic ordering temperature in $\text{Yb}_2\text{Fe}_3\text{Si}_5$.

B. Resistivity studies

The temperature dependence of the resistivity (ρ) data of $\text{Yb}_2\text{Fe}_3\text{Si}_5$ is shown in Fig. 4. The two insets (a) and (b) display the ρ behavior from 1.4 to 5 K and 1.4 to 50 K, respectively. The large value of the $\rho(T)$ at room temperature and a low value of the residual resistivity ratio down to

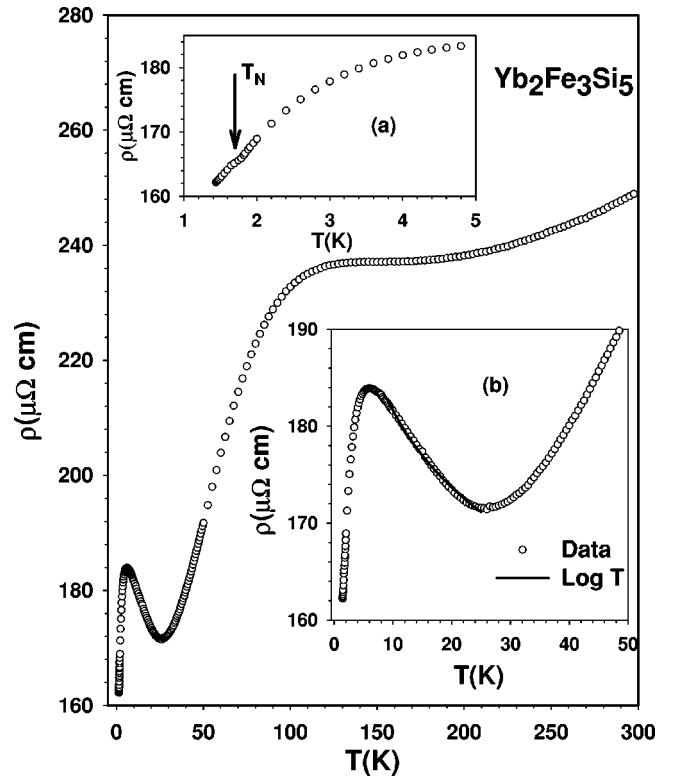


FIG. 4. Temperature dependence of the resistivity (ρ) of $\text{Yb}_2\text{Fe}_3\text{Si}_5$ from 2 to 300 K. The inset (a) shows the ρ data from 1.4 to 5 K on an expanded scale whereas the inset (b) shows ρ data up to 50 K. A small kink which is marked by an arrow in the inset (a) indicates antiferromagnetic ordering of Yb^{3+} moments, which is in agreement with the χ data. The solid line shown in the inset (b) is a fit to the $\log T$ dependence (see text).

5 K could be due to either the structural disorder (intersite change between Fe and Si) or to the strong hybridization effects. It must be recalled here that the properties of the 2-3-5 silicides are highly anisotropic¹⁵ and the over all shape of the temperature dependence of $\rho(T)$ of a polycrystal can easily be influenced by the anisotropy. The important aspect is the the low-temperature ρ data on an expanded scale as shown by the inset (b). From this inset one can clearly see the nonmonotonic dependence of $\rho(T)$ with a $\log T$ dependence from 9 to 25 K. The low-temperature ρ data below 30 K display a typical Kondo lattice response with a minimum at 25 K followed by a maximum of $\rho(T)$ at 6 K. Subsequently, $\rho(T)$ falls sharply below 4.5 K due to coherence. A small kink in the resistivity data at 1.7 K [shown in panel (a)] indicates a possible magnetic transition at 1.7 K, which is in agreement with the susceptibility data.

C. Heat-capacity studies on $\text{Yb}_2\text{Fe}_3\text{Si}_5$

The temperature-dependent C_p data from 0.4 to 25 K of $\text{Yb}_2\text{Fe}_3\text{Si}_5$ is shown in the top panel (a) of Fig. 5. The inset in this panel describes the low temperature behavior which emphasizes the sharpness of the antiferromagnetic transition. The large jump (~ 4 J/mol K) at T_N clearly shows bulk magnetic ordering of Yb^{3+} moments. The antiferromagnetic

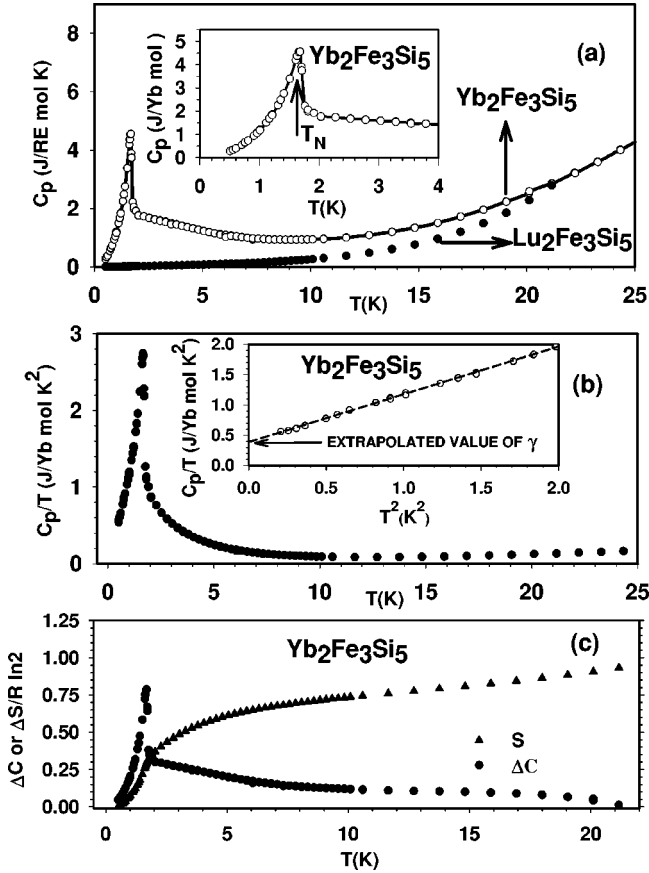


FIG. 5. Plot of the heat-capacity (C_p) vs temperature (T) of $\text{Yb}_2\text{Fe}_3\text{Si}_5$ from 0.3 to 25 K. The inset in the top panel (a) shows the low-temperature C_p data on an expanded scale. Plot of C/T vs T is displayed in the middle panel (b) which gives an upper limit for the value of γ as 0.5 J/Yb mol K^2 and the inset shows the extrapolated $\gamma(0)$ (0.4 J/Yb mol K^2) value using C/T vs T^2 plot. The bottom panel (c) depicts the magnetic contribution to the heat capacity (after subtracting the lattice contribution estimated from the C_p data of $\text{Lu}_2\text{Fe}_3\text{Si}_5$) and the estimated entropy in this temperature range.

ordering temperature obtained from the heat capacity measurements is in accordance with those obtained from the χ and ρ measurements. The specific heat data of $\text{Lu}_2\text{Fe}_3\text{Si}_5$ in the normal state is also shown in the same panel.

In the second panel of Fig. 5, the temperature dependence of C/T data are shown. Well below T_N these data can be nicely fitted with a linear and a cubic term $C = \gamma T + \beta T^3$, as shown in the inset. The cubic term in this case corresponds to the contribution of antiferromagnetic magnons, since the phonons are completely negligible in this temperature range. The linear term obtained from this extrapolation, $\gamma = 0.4$ J/Yb mol K^2 , can be considered as a lower limit for the Sommerfeld coefficient, since the experimental data show an upward curvature at the lowest limit of the measurement. This would indicate freezing out of the magnons due to an anisotropy gap. In this case, $C/T = 0.5$ J/Yb mol K^2 at the lowest measured temperature gives the upper limit for this Sommerfeld coefficient. The magnetic contribution to the heat capacity of $\text{Yb}_2\text{Fe}_3\text{Si}_5$ (which is obtained after sub-

tracting the C_p data of $\text{Lu}_2\text{Fe}_3\text{Si}_5$) is shown in the third panel (c) of the Fig. 5. The estimated entropy from the experiment is also shown in the same panel. The entropy is nearly temperature independent from 7 to 12 K and reaches a value of $0.9R \ln 2$ (R is the gas constant) at 20 K, which establishes that the ground state is a well separated doublet. The heat capacity also shows a small negative curvature above 1.8 to about 3 K. There are two possibilities for the tail in C_p above T_N : short range fluctuations or Kondo effect. We would argue that the sharpness of the transition and the weak T dependence of C/T above T_N are in disagreement with short range correlations, whereas the Kondo scenario is supported by the resistivity maximum at 6 K and the large γ value. Moreover, the entropy at T_N [$S_{\text{mag}} = S(T_N)$] is found to be $0.39R \ln 2$, which strongly indicates that the ordered moment is heavily compensated by Kondo interactions. In the absence of short range order, the reduction in S_{mag} at T_N is due to the partial lifting of the twofold degeneracy of the ground state above T_N by Kondo effect. In such cases, one can show that $S_{\text{mag}} = S_K(T_N/T_K)$, where $S_K(t)$ is the entropy of a single ion Kondo impurity at the normalized Kondo temperature $t = T_N/T_K$.¹⁶ The entropy has been calculated by Desgranges and Schotte using the Bethe ansatz for a spin-1/2 Kondo model.¹⁷ Sharp heat capacity anomaly at T_N and the possible absence of short range order facilitate the use of the theory¹⁷ and with the experimental value of S_{mag} , we estimate a value of 5 K for the Kondo temperature of $\text{Yb}_2\text{Fe}_3\text{Si}_5$. However, accurate estimation requires inelastic scattering data. The value of the entropy at 20 K is only $0.9R$ which is much smaller than the theoretical value of $2.08R$ [$R \ln(2J + 1)$ with $J = 7/2$ for the free Yb^{3+} ion]. This indicates that the CEF levels are well splitted by the tetragonal symmetry.

IV. CONCLUSION

To conclude, we have observed antiferromagnetic ordering and heavy electron behavior in $\text{Yb}_2\text{Fe}_3\text{Si}_5$ using resistivity, magnetization, and heat capacity studies. It is interesting to note that both $\text{Lu}_2\text{Fe}_3\text{Si}_5$ and $\text{Tm}_2\text{Fe}_3\text{Si}_5$ are superconducting at 6.2 and 1.2 K, respectively, while the Yb sample did not show superconductivity down to 100 mK. It should be noted here that the superconducting $\text{Tm}_2\text{Fe}_3\text{Si}_5$ compound becomes reentrant antiferromagnet at 1.1 K and remains in the same state down to 50 mK. We believe that the absence of superconductivity in Yb sample is due to the Kondo effect, which is quite strong in suppressing the superconductivity. The magnetic ordering temperature of $\text{Yb}_2\text{Fe}_3\text{Si}_5$ is also higher than that of the Tm compound which implies an enhanced exchange in the former. Here, it is the Fe neighbors, which provide a very strong $d-f$ hybridization, and the Si neighbors, which provide a significant $p-f$ hybridization. In view of the large effect of pressure on the properties of $\text{Tm}_2\text{Fe}_3\text{Si}_5$, similar studies are essential on $\text{Yb}_2\text{Fe}_3\text{Si}_5$ to induce superconductivity via quenching of the Kondo effect. Such studies are in progress and will be reported elsewhere.

- ¹P. Rogl in *Handbook of Physics and Chemistry of Rare Earths*, edited by K.A. Gschneidner, Jr. and L. Eyring (Elsevier Science Publishers, North-Holland, Amsterdam, 1984), Vol. 7, pp. 1–264.
- ²J. Leciejewicz and A. Szytula, in *Handbook of Physics and Chemistry of Rare Earths*, edited by K.A. Gschneidner, Jr. and L. Eyring (Elsevier Science Publishers, Amsterdam, 1989), Vol. 12, p. 133.
- ³H.F. Braun, *J. Less-Common Met.* **100**, 105 (1984).
- ⁴R.N. Shelton, in *Proceedings of the International Conference on Superconductivity in d- and f- band Metals*, edited by W. Buckel and W. Weber (Kernforschungszentrum, Karlsruhe, Germany, 1982), p. 123.
- ⁵H.F. Braun, *Phys. Lett.* **75A**, 386 (1980).
- ⁶H.F. Braun, C.U. Segre, F. Acker, M. Rosenberg, S. Dey, and U. Deppe, *J. Magn. Magn. Mater.* **25**, 117 (1981).
- ⁷A.R. Moodenbaugh, D.E. Cox, and H.F. Braun, *Phys. Rev. B* **25**, 4702 (1981).
- ⁸C.B. Vining and R.N. Shelton, *Phys. Rev. B* **28**, 2732 (1983).
- ⁹H.F. Braun, in *Ternary Superconductors*, edited by G.K. Shenoy, B.D. Dunlap, and F.Y. Fradin (North-Holland, Amsterdam, 1980), p. 225.
- ¹⁰J.A. Gotaas, J.W. Lynn, R.N. Shelton, P. Klavins, and H.F. Braun, *Phys. Rev. B* **36**, 7277 (1987).
- ¹¹S. Noguchi and K. Okuda, *Physica B* **194-196**, 1975 (1994).
- ¹²FULLPROF x-ray powder diffraction program available at Collaborative Computational Project Number 14 (CCP14), URL www.ccp14.ac.uk
- ¹³S. Ramakrishnan, S. Sundaram, R. S. Pandit, and Girish Chandra, *J. Phys. E* **18**, 650 (1985).
- ¹⁴P.G. de Gennes, *J. Phys. Radium* **23**, 510 (1962).
- ¹⁵B. Becker, S. Ramakrishnan, A. A. Menovsky, G. J. Nieuwenhuys, and J. A. Mydosh, *Phys. Rev. Lett.* **78**, 1347 (1997). See also Ref. 11.
- ¹⁶K. Satoh, T. Fujita, Y. Maeno, Y. Uwatoko, and H. Fujii, *J. Phys. Soc. Jpn.* **59**, 692 (1990).
- ¹⁷H. U. Desgranges and K. D. Schotte, *Phys. Lett.* **91A**, 240 (1982).